PAPERS

Fe_3S_4 and Fe_3O_4 magnetic nanocrystals: magneto-optical and Mössbauer spectroscopy study

To cite this article: C-R Lin *et al* 2014 *Mater. Res. Express* **1** 025033

Materials Research
Express

Fe_3S_4 and Fe_3O_4 magnetic nanocrystals: magneto-optical and Mössbauer spectroscopy study

C-R Lin[1], Y-T Tseng[1], S G Ovchinnikov[2,3], R D Ivantsov[2], I S Edelman[2], A S Fedorov[2,3], A A Kuzubov[3], D A Fedorov[4], S S Starchikov[5] and I S Lyubutin[5]

[1] Department of Applied Physics, National Pintung University of Education, Pintung 90003, Taiwan
[2] L.V. Kirensky Institute of Physics, Siberian Branch of Russian Academy of Sciences, Krasnoyarsk, 660036, Russia
[3] Siberian Federal University, Krasnoyarsk, 660041, Russia
[4] University of Nevada, Reno, NV 89557, USA
[5] Shubnikov Institute of Crystallography, Russian Academy of Sciences, Moscow 119333, Russia
E-mail: crlin@mail.npue.edu.tw and sgo@iph.krasn.ru

Received 12 March 2014, revised 17 April 2014
Accepted for publication 24 April 2014
Published 4 June 2014
Materials Research Express **1** (2014) 025033
doi:10.1088/2053-1591/1/2/025033

Abstract

Iron oxide magnetite (Fe_3O_4) should be a reasonable analog for conception and understanding of the magnetic properties of iron sulfide greigite (Fe_3S_4)—one of the most required magnetic materials having numerous applications but being far from the complete understanding now. We present here a comparative study of the Mössbauer effect (ME) and the magnetic circular dichroism (MCD) spectroscopy of Fe_3O_4 and Fe_3S_4 nanoparticles. The ME spectrum parameters of Fe_3S_4 are shown to distinguish strongly from that of Fe_3O_4, and the MCD spectrum shapes are shown to be absolutely different for two compounds. To clarify the origin of the Fe_3S_4 MCD spectrum we have performed *ab initio* band structure calculations and identified the MCD spectrum features with the transitions between calculated energy states.

Keywords: iron sulfide Fe_3S_4, iron oxide Fe_3O_4, magnetic nanoparticles, Mössbauer spectroscopy, magnetic circular dichroism, *ab-initio* band structure calculations

1. Introduction

The constantly increasing interest to the nanoscale magnetic particles is due to their physical and chemical properties being promising for applications in many fields (see, for instance,

reviews [1–3] and references therein). Among them, the nanoparticle-based composites are considered as promising candidates for data storage, high-performance luminescence and laser beam processing devices. In this connection, an enhancement of the optical and magneto-optical efficiency of magnetic nanocomposites is one of the main goals of nanotechnology. Great attention has been paid, for example, to the ferrite [4, 5] and Eu chalcogenide [6–9] nanoparticles. Iron chalcogenides could be of interest for the magneto-optical applications as well. Iron sulfide Fe_3S_4, greigite, one of the representatives of this system, allomeric to the iron oxide magnetite, Fe_3O_4, was outside magneto-optical study up to now. At the same time, both compounds, Fe_3O_4 and Fe_3S_4 are the most commonly studied magnetic materials having numerous applications. Fe_3O_4 has been known and applied from ancient times, whereas greigite was not formally reported until 1964 when it was defined as a mineral from the Californian lacustrine sediments by Skinner *et al* [10]. Since then, the number of publications devoted to the properties of greigite has grown rapidly because of its importance in palaeomagnetism, environmental, biological, biogeochemical, tectonic, and industrial processes (e.g., see review [11] and references therein). Both, magnetite and greigite crystallize in the inverse spinel structure (space group *Fd3m*) with parameters $a = 8.396$ Å [12] and $a = 9.83$–9.90 Å [13], respectively. They have the same cation distribution (Fe^{3+}) $[Fe^{3+}Fe^{2+}]$ X_4 (X = O, S), where parentheses and square brackets refer to the tetrahedral (A) and octahedral [B] sites, respectively. Despite structural similarities between the two compounds, their magnetic properties are different in many aspects. According to [13], the room temperature saturation magnetization of greigite is of 3.13 μ_B per formula unit (f.u.) increasing to 3.35 μ_B/f.u. at 5 K due to decreased thermal excitation. Meanwhile, the room temperature saturation magnetization of magnetite is noticeably higher −4.0 μ_B/f.u., and it corresponds to the value expected from a purely ionic model [14]. The exchange parameter J_{AB} between tetrahedral and octahedral magnetic sub-lattices in greigite was estimated recently as ~1.03 meV [13], which is lower than the J_{AB} value calculated for magnetite (2.88 meV) [15]. Nevertheless, magnetite should be a reasonable analog for conception and understanding of the magnetic properties of greigite, which are far from completely understood. The authors of [16] have devoted their efforts to the comparative study of the magnetic properties of greigite and magnetite nanocrystals synthesized by the hydrothermal method. They have compared the magnetization curves and field cooled (FC) and zero field cooled (ZFC) magnetization temperature dependences of these two compounds. Recently, elastic constants and other macroscopic mechanical properties as well as the electronic properties of Fe_3S_4 and Fe_3O_4 have been calculated in [17], using the *ab initio* method based on spin-polarized density functional theory with the on-site Coulomb repulsion approximation. The sulfide Fe_3S_4, has been shown to be more covalent than the oxide, Fe_3O_4, and the density of states (DOS) of Fe_3S_4 has appeared to be more complex since the less electronegative S bands are positioned at higher energies compared to the oxygen bands in Fe_3O_4. The electronic structure differences between these two compounds should affect many physical properties. That is why further comparative study of the Fe_3S_4 and Fe_3O_4 compounds and, especially, in the nanostructured state seems to be rather productive.

Mössbauer effect (ME) and magneto-optical (MO) spectroscopy are appropriate methods for such a comparison as they are expected to yield consistent and complementary data. ME provides information on the magnetic and structural properties of a substance including the iron ions (valence and distribution over magnetic sub lattices), while MO allows studying the electron transitions between energy levels of ions occupying different crystal sites. Mössbauer spectroscopy was applied recently [18, 19] for monitoring of the Fe_3O_4 nanoparticles synthesis

by the thermal reduction of hematite α-Fe_2O_3 powder in the presence of high boiling point solvent. The quantitative content of hematite and magnetite phases was evaluated at each step of the chemical and thermal treatment of the product. It was established from the Mössbauer data that not all iron ions in the octahedral *B*-sites of magnetite nanoparticles participate in the electron hopping $Fe^{2+} \rightleftarrows Fe^{3+}$ above the Verwey temperature T_V, which can be explained by surface effects [19]. It was shown that the surface effects, influencing the electronic states of iron ions, dominate the vacancy effect, and thus govern the observed specific features of the Verwey transition and magnetic properties.

The recent Mössbauer study of iron sulfide nanoparticles Fe_3S_4 [20] revealed an occurrence of the cation vacancies in small particles (9 nm) of the nonstoichiometric greigite. The stoichiometric phase of greigite dominates in the 18 nm size nanoparticles. The Mössbauer parameters indicate a great degree of covalence in the Fe-S bonds and support the fast electron $Fe^{3+} \rightleftarrows Fe^{2+}$ exchange in the B-sites of greigite. An absence of the Verwey transition at temperatures between 90 and 300 K was established and it was explained by a semimetal type of conductivity [20].

Like other magnetic properties, the magneto-optical effects in Fe_3O_4 have been studied by many authors. Most attention was paid to the Kerr rotation (KR) and Kerr ellipticity (KE) measured both for polished crystals and thin films (see [21–25] and references therein). The Faraday rotation (FR) measurements in magnetite nanoparticles of different size embedded in polymethyl methacrylate matrix were presented in [26, 27]. Bases on the Faraday ellipticity (FE) and FR measurements in the Fe_3O_4 thin films, the authors of [28, 29] have calculated the dielectric tensor off-diagonal components ε'_{xy} and ε''_{xy}, and used their spectral and temperature dependences to detect the Verwey phase transition and to describe the Fe_3O_4 electronic band structure. Contrary to the situation with Fe_3O_4, we have managed to find only one paper [30] in the literature where the magneto-optical effect was mentioned, namely Kerr effect, which was used to detect domain structure in greigite sample. Quite recently, we have presented our first observations of magnetic circular dichroism (MCD) measured in the transmitted light in greigite nanoparticles dispersed in transparent dielectric matrix [20]. The MCD technique is one of the particularly informative magneto-optical effects [31], as far as it is observed in the relatively narrow bands at photon energies corresponding to transitions between ground and excited states of an ion in insulators or between bands in metals and semiconductors. Characteristics of MCD spectra are helpful for in-depth understanding of the nanoparticles electronic structure and electronic excitations under the action of electromagnetic irradiation.

The present paper is devoted to the comparative study of Mössbauer effect and MCD in the Fe_3S_4 and Fe_3O_4 nanoparticles dispersed in non-magnetic matrices. Identification of the resonances in the Fe_3S_4 MCD spectrum is made with the electronic transitions between energy states obtained by the *ab initio* band structure calculations.

2. Experiment

The process of synthesis, structural and magnetic properties of the Fe_3S_4 and Fe_3O_4 nanoparticles were described in our previous publications [18, 20]. The samples were characterized by x-ray powder diffraction (XRD), transmission electron microscopy (TEM), and ^{57}Fe-Mössbauer spectroscopy. The reflections in XRD patterns were indexed to the cubic phase with spinel-type structure (space group $Fd\bar{3}m$). The estimation of the average crystallite

size was made by the Scherrer's formula from the XRD-peak broadening. For the present studies, the monodispersed powders, according to the TEM images, of the Fe_3S_4 (20 nm size) [20] and Fe_3O_4 (40 nm size) [32] nanoparticles were used.

Transparent silicon-based glue 'Rayher' (art. nr. 3338 100 80 ml) was chosen as a material for the matrix. The particles powder was stirred into it. The obtained composite was placed between two polished glass plates spaced with two wires of 0.15 mm in thickness. After solidification, the samples were transparent in the visible spectral range.

The MCD spectra were measured using the modulation of the light polarization state with a piezoelectric modulator. The modulator consisted of the piezoelectric ceramic element pasted on the plate of fused silica. The modulator was a part of the self-contained generator and oscillated with its resonance frequency of about 25 kHz. The light beam from the filament lamp, passing through the polarizer and then through the modulator, became circularly polarized and the light polarization changed from the right to the left circular one with the resonance frequency of the modulator. The circularly polarized light, passing through the sample placed between magnetic poles, acquired a modulation of its intensity due to circular dichroism of the sample. The MCD effect was measured with a relative accuracy of 10^{-4} as a difference in photomultiplier signals (proportional to the light intensity change) obtained at magnetic field applied along and opposite to the light direction. Azimuthal modulation of the polarization plane orientation of the incident light wave was used for the FR measurement with an accuracy of ±0.2 min. FR and MCD were measured in the spectral range 1.2–3.5 eV at temperatures 88 and 298 K. Magnetic field was directed normally to the sample (planar matrix containing the nanoparticles) plane. Because the method of the samples preparation does not allow the precise measurement of the nanoparticles concentration in a sample and the sample thickness, the magneto-optical effect values will be given here in arbitrary units.

3. Results and discussion

3.1. The comparative Mössbauer spectra of Fe_3O_4 and Fe_3S_4 nanoparticles

The comparative ^{57}Fe-Mössbauer spectra of Fe_3O_4 and Fe_3S_4 nanoparticles at room and liquid nitrogen temperatures are shown in figure 1. All spectra have revealed Zeeman magnetic splitting indicating the magnetic ordering state of Fe ions in the 80–300 K temperature intervals. However, even qualitative difference of the Fe_3O_4 and Fe_3S_4 spectra is obvious. Two six-line magnetic patterns in the Fe_3O_4 spectrum at room temperature originate from iron ions in the tetrahedral (A) and octahedral [B] magnetic sub-lattices. The Fe_3O_4 spectrum drastically changes when temperature decreases to 80 K, which effectively demonstrates the Verwey transition (see details in [18]). The estimated value of the Verwey point in this sample is 136 K [18].

In the Mössbauer spectra of greigite, the (A) and [B] magnetic sub-lattices are not clearly resolved, and the spectra shape does not sufficiently change with temperature lowering from 300 to 90 K (figure 1). The shape of Mössbauer spectra of Fe_3S_4 and the hyperfine parameters indicate an absence of the Verwey transition at temperatures between 90 and 300 K. This was also supported by the magnetization measurements [18, 20]. Contrary to magnetite, the Mössbauer spectra of greigite do not distinguish the Fe^{2+} and Fe^{3+} ions in B-sites at both 300 and 90 K thus supporting the fast electron $Fe^{3+} \rightleftarrows Fe^{2+}$ exchange.

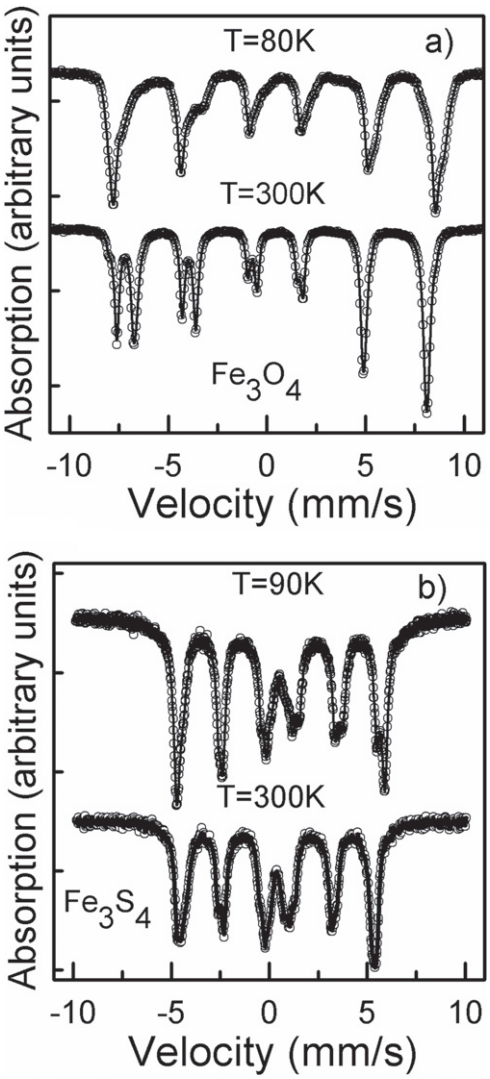

Figure 1. The ^{57}Fe-Mössbauer spectra of magnetite Fe_3O_4 and greigite Fe_3S_4 nanoparticles at room and nitrogen temperatures. Redistribution of the line intensities in the left-hand part of the magnetite spectra with temperature reveals the Verwey phase transition.

As seen in figure 1, the total Zeeman splitting of the resonance lines in the Mössbauer spectra of magnetite is much larger than in greigite. It indicates that the magnetic hyperfine fields H_{hf} at iron nuclei in oxide are essentially larger than in sulfide. The hyperfine parameters obtained from the Mössbauer spectra of magnetite and greigite nanoparticles are given in table 1.

The values of magnetic hyperfine fields H_{hf} at iron nuclei in greigite are close for octahedral and tetrahedral sites and are in the range of (31.9–30.0) T at temperatures between 90 and 300 K (table 1). The hyperfine field H_{hf} in the B-sites is somewhat lower than in the A-sites and this is consistent with the iron valence states [20]. These H_{hf} values in sulfide are much lower than in oxides (typically 50–55 T at low temperatures) which is explained by delocalization of d-electrons in sulfides with reduction of the ionic magnetic moment of iron.

Table 1. Hyperfine parameters obtained from the ^{57}Fe-Mössbauer spectra at 300 K for the nanoparticles of greigite Fe_3S_4 and magnetite Fe_3O_4: H_{hf} is the magnetic hyperfine field at ^{57}Fe nuclei, δ is the isomer shift relative to α-Fe, ε is the quadruple shift, Γ is the half maximum line width, and S is the relative line area of the spectrum component.

Iron component from Mössbauer spectra	H_{hf}, T (±0.2)	δ, mm s^{-1} (±0.01)	ε, mm s^{-1} (±0.01)	Γ, mm s^{-1} (±0.02)	S% (±2)
		Fe_3S_4			
Fe^{3+} in A-sites	30.9	0.27	−0.01	0.29	22
(Fe^{2+} + Fe^{3+}) in B-sites	30.0	0.53	0.09	0.57	42
		Fe_3O_4			
(Fe^{3+}) in A-sites	49.0	0.28	0.00	0.28	36
(Fe^{3+} + Fe^{2+}) in B-sites	45.8	0.67	0.00	0.41	58

The isomer shifts are generally rather smaller in sulfides than in oxides on account of the greater degree of covalence in the Fe–S bonds. In particular, the δ values in both A- and B-sites of greigite Fe_3S_4 are smaller than the corresponding values in oxide Fe_3O_4. In our stoichiometric Fe_3S_4 nanoparticles, the A-site isomer shift $\delta(300\,\mathrm{K}) = 0.27\,\mathrm{mm\,s^{-1}}$ suggests that the iron in these sites is predominantly ferric. The B-site isomer shift value $\delta\left(300\,\mathrm{K}\right) = 0.52\,\mathrm{mm\,s^{-1}}$ in greigite and $0.67\,\mathrm{mm\,s^{-1}}$ in magnetite are quite consistent with the presence of both ferric and ferrous ions on these sites, if one assumes that fast electronic exchange occurs between the two species [33, 34]. Due to the fast electron hoping between Fe^{2+} and Fe^{3+} ions in the B-sites, the average iron valence of near $Fe^{2.5+}$ is seen in the Mössbauer spectra:

$$\left(\mathrm{Fe}^{3+}\right)_{\mathrm{tet}}\left[\mathrm{Fe}^{3+}\,\mathrm{Fe}^{2+}\right]_{\mathrm{oct}}\mathrm{X}_4 = \left(\mathrm{Fe}^{3+}\right)_{\mathrm{tet}}\left[\mathrm{Fe}^{22.5+}\right]_{\mathrm{oct}}\mathrm{X}_4, \quad \left(\mathrm{X} = \mathrm{O\ or\ S}\right)$$

This electronic state maintains at all temperatures between 90 and 300 K in greigite, but only at $T > T_V = 136$ K in magnetite. Below T_V, the electron hoping in magnetite freezes, and the iron valence state becomes stable as $(Fe^{3+})_{tet}[Fe^{3+}\ Fe^{2+}]_{oct}O_4$.

3.2. Magneto-optical experimental data

The MCD and FR dependences on an external magnetic field of the samples containing Fe_3S_4 and Fe_3O_4 nanoparticles coincide in shape with the magnetization field dependences of these nanoparticles powder presented in [20] and [18], respectively. Such a coincidence seems to be natural as MCD and FR are the magneto-optical effects linear in the sample magnetization. As an example the, Fe_3S_4 hysteresis loop is shown in figure 2. The MCD spectral dependences for the samples containing Fe_3S_4 and Fe_3O_4 nanoparticles recorded at the magnetic field of 3.0 kOe are shown in figure 3(a) for two temperatures. Two extremes of the opposite signs observed at about 1.8 and 2.7 eV dominate in the whole visible part of the Fe_3O_4 nanoparticles MCD spectrum. Similar extremes were observed at about 2 eV and 3 eV in the Kerr rotation (KR) spectrum of the bulk Fe_3O_4 polished sample [23]. Such a coincidence is not surprising because both effects: MCD $\left(\theta_F\right)$ and KR $\left(\theta_K\right)$ are described by the similar equations [35]

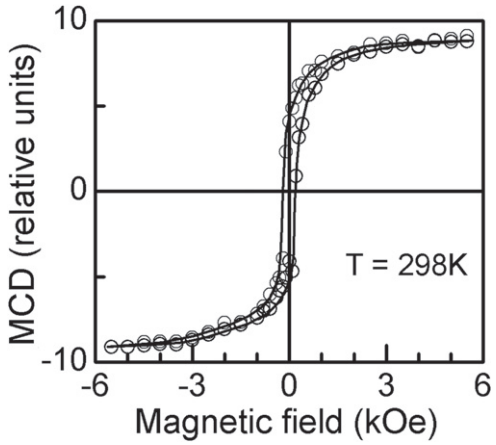

Figure 2. Room temperature MCD versus external magnetic field for sample containing Fe_3S_4 nanoparticles, E = 2.3 eV.

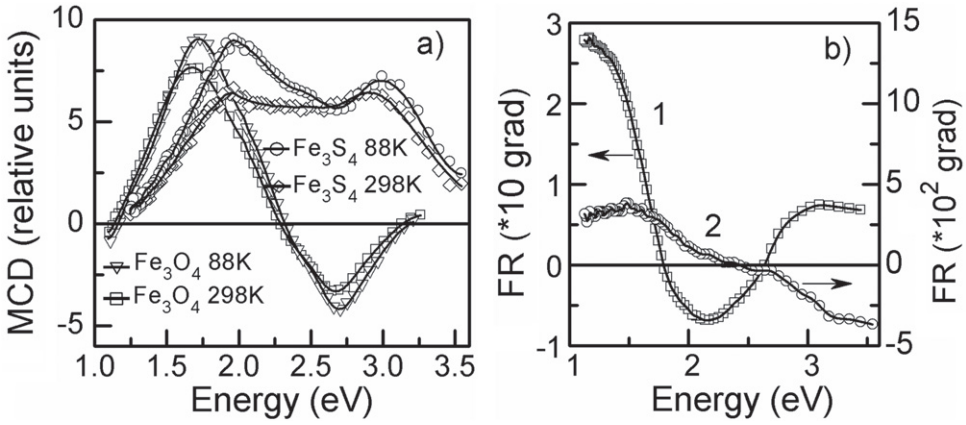

Figure 3. (a) MCD spectra of Fe_3S_4 and Fe_3O_4 nanoparticles at temperatures 298 K (diamonds and squares, correspondingly) and 88 K (circles and triangles, correspondingly); (b) FR spectra of Fe_3O_4 (curve 1) and Fe_3S_4 (curve 2) nanoparticles at temperature 298 K, $H = 3$ kOe.

$$\theta_F = \frac{4\pi}{\lambda}\left\{\frac{n}{k^2+n^2}\varepsilon''_{xy} - \frac{k}{k^2+n^2}\varepsilon'_{xy}\right\},$$

and

$$\theta_K = \frac{B}{B^2-A^2}\varepsilon''_{xy} - \frac{A}{B^2-A^2}\varepsilon'_{xy},$$

where ε'_{xy} and ε''_{xy} are the real and imaginary parts of the off-diagonal component of the dielectric tensor, n and k are the refractive index and absorption coefficient, respectively, λ is the light wave length, $A = (n^3 - 3nk^2 - n)$ and $B = (3n^2 - k^3)$. The extreme positions in the MCD spectrum of Fe_3O_4 coincide with the points where FR signal crosses zero line in the FR spectrum (figure 3(b)). This corresponds to the well-known Kramers–Kronig equations [36, 37]. Similar

behavior of the FR spectrum was observed in the magnetite-polymer nanocomposites containing Fe_3O_4 nanoparticles of 30 nm in size [22]. In our sample, both the positive and negative extreme amplitudes of the MCD spectra increase slightly with temperature decrease (figure 3(a)). It is worth noting that the Verwey transition does not reflect in the shape of the Fe_3O_4 MCD spectra, it could be evidence of the same origin of the electron transitions responsible for the magneto-optical effects in the whole temperature interval.

In spite of the same structure and iron ion distributions among crystal positions, the magneto-optical spectra of Fe_3S_4 distinguish drastically from that of Fe_3O_4 (see figures 3(a) and (b)). A very vide 'bell'-shaped curve with two local maxima and a valley between them characterizes the MCD spectrum (figure 3(a)).

Evidently, such a shape should be due to the overlap of several peaks. The FR curve of Fe_3S_4 passes through zero at the energy corresponding approximately to the gravity center of the 'bell' (compare figures 3(a) and (b)). Several details in the MCD spectrum attract our attention:

(i) an absence of the negative peak observed in the MCD spectrum of Fe_3O_4;

(ii) the maximum values of the MCD signal at energies near 2.0 eV and 3.0 eV increase in different way with cooling the sample from 298 to 88 K;

(iii) a small decrease of the MCD signal in the valley region at 2.65–2.85 eV with the temperature lowering.

In order to extract meaningful information from the MCD data, we have carried out the MCD spectra decomposition to several Gauss components for the Fe_3O_4 (figure 4(a)) and Fe_3S_4 (figure 4(b)) nanoparticle ensembles.

The best fitting in the case of magnetite, we obtained introducing a peak centered at $E < 1.0$ eV which is not observed experimentally here. The necessity to account for this peak was proved by observation of the Kerr effect peak at this energy [22]. Parameters of the decomposition components best fitted to experimental data for Fe_3O_4 and Fe_3S_4 are collected in table 2. Both peaks—positive and negative—in the visible Fe_3O_4 MCD spectrum can be compared with the resonances at 1.94 and 2.61 eV in the ε''_{xy} spectrum of the Fe_3O_4 single crystal obtained from the Kerr effect measurements in [21]. Based on the spectral maxima changes when substituting Fe ions by Mg^{2+} and Al^{3+}, the authors of [21] ascribed the first of these peaks to the intervalence charge transfer (IVCT) transition $t_{2g} \rightarrow e_g$ between $[Fe^{2+}]$ and $[Fe^{3+}]$, and the second one to the inter sub-lattice charge transfer (ISCT) $t_2 \rightarrow t_{2g}$ transition between (Fe^{3+}) and $[Fe^{2+}]$ ions.

Going to the decomposition of the greigite MCD spectrum, one can see two wide intensive positive peaks E1 and E3 and weak negative peak E2. So, we found the qualitative difference between sets of peaks in the MCD spectra of Fe_3O_4 and Fe_3S_4 which have revealed the different nature of electron transitions in magnetite and greigite. In the next section we will confirm this statement analyzing the band structure and DOS in greigite.

3.3. Electronic structure of greigite and origin of the MCD spectrum

To clarify the origin of the Fe_3S_4 MCD spectra we have performed the *ab initio* band structure calculations by the pseudo-potential method using the plane wave basis within the density functional theory (DFT) [38, 39] in the generalized gradient approximation (GGA), version

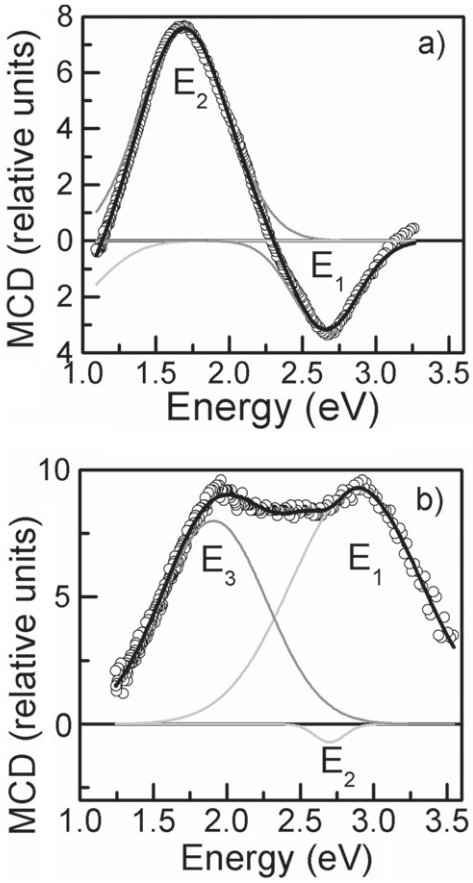

Figure 4. (a) The Fe_3O_4 MCD spectrum decomposition to the components of the Gauss shape—E_1 and E_2 (E_3 is beyond the graph) and (b) The Fe_3S_4 MCD spectrum decomposition to three components of the Gauss shape E_1, E_2, and E_3. Bold black lines are the sums of three components, gray lines are the components, and circles are the experimental data.

Table 2. Parameters of the Gauss shape components best fitted to the experimental MCD curves at temperatures 298 and 88 K. E_0 is the gravity center energy, A is the amplitude (intensity), ΔE is the half-width, and S is the area of each component.

E_0, eV	A* 10^4	ΔE, eV	S* 10^4	E, eV	A* 10^4	ΔE, eV	S* 10^4	A_{88K}/A_{298K}	S_{88K}/S_{298K}
$T = 298$ K				$T = 88$ K					
				Fe_3O_4					
2.6	−46	0.32	46	2.65	−54.3	0.30	51	1.18	1.11
1.68	88	0.42	117	1.73	102	0.39	124	1.16	1.06
1.06	−33	0.31	32	0.99	−36	0.37	42	1.09	1.31
				Fe_3S_4					
2.88	9.21	0.52	10	2.98	9.84	0.43	9,40	1.07	1.06
2.70	−0.71	0.12	0.18	2.75	−1.1	0.11	0.28	1.63	1.63
1.91	8.00	0.43	7.27	1.98	11.9	0.32	11.0	1.48	1.53

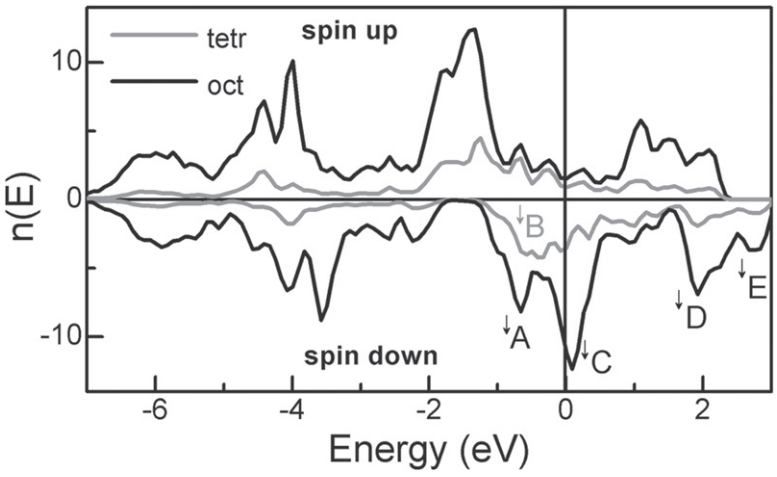

Figure 5. Site resolved spin polarized electron DOS in Fe_3S_4 for octahedral (black lines) and tetrahedral (gray lines) positions. Down arrows correspond to the spin 'down' states. The Fermi level is at $\epsilon_F = 0$. Different peaks in DOS relevant for the interband transitions and formation of the MCD spectrum are denoted by indexes like A, B, C, D, E.

PW91 [40]. We have used the VASP 5.2 (Vienna *ab initio* Simulation Package) code [41, 42] with the ultra-soft Vanderbilt potential [43]. The cutoff energy was taken 280 eV. The integration over the first Brillouin zone was carried out using the Monkhorst–Pack scheme with $(2 \times 2 \times 1)$ grid [44]. The crystal structure with 24 Fe atoms and 32 S atoms in the unit cell with the lattice parameter $a = 0.973$ nm and magnetic moment per formula unit $\mu = 3.25\ \mu_B$ have been optimized by the spin polarized GGA+U method with the Hubbard correction $U = 2.5$ eV. Spin polarized band structure and DOS of the bulk Fe_3S_4 have revealed the metal state with the dominant *d* electron contribution at the Fermi level. The spin polarized DOS is shown in figure 5 for two atomic positions (octa- and tetrahedral sites of Fe_3S_4). The dominant contribution at the Fermi level $\epsilon_F = 0$ results from the spin down *d*-electrons marked as $B^{\downarrow}$ peak (figure 5) originated from the octahedral position.

Previously the greigite band structure has been calculated by different approximations of the density functional theory, the GGA+U [17, 45] and LAPW [46] methods with different results. The half-metallic band structure of greigite [45] is similar to magnetite [24, 47]. In contrast, the metallic properties of greigite with two Fermi surfaces for spin up and spin down electrons and unusually strong spin-orbital interaction has been found in [46]. Our DOS in figure 5 reveals the small contribution of the anion electrons and dominant contribution of the B-site Fe spin down electrons at the Fermi level similar to [45]. Contrary to [45] and in agreement with [46] we have obtained the metallic state with a small contribution of the spin up projection at the Fermi level. In addition, small but not negligible contributions from the spin polarized electrons of the A-site Fe ions should be taken into account (figure 5). The metal state of greigite contrary to the half-metal state of magnetite excludes the Verwey transition, as was also mentioned in [47]. Indeed, our Mössbauer spectroscopy and magnetic measurements in greigite give no indication for the Verwey transition [20]. Using the calculated spin- and site dependent DOS of the greigite we may at least qualitatively analyze the MCD spectra. The

Table 3. Comparison of the experimental MCD peak positions with the possible interband excitations.

Experimental peak position and width, $T = 298$ K		
E, eV	ΔE, eV	Interband excitations and corresponding energies (in brackets)
2.88	0.45	$\downarrow A \rightarrow \downarrow D$ (3.0 eV) + $\downarrow C \rightarrow \downarrow E$ (2.8 eV)
2.70	0.11	$\downarrow B \rightarrow \downarrow D$ (2.5 eV)
1.91	0.43	$\downarrow C \rightarrow \downarrow D$ (1.9 eV)

MCD spectrum is formed by the interband excitations from the occupied to the empty electronic states with the same spin projections.

The energies of different interband excitations have been calculated from figure 5 and compared with energies of the MCD resonances obtained from the its spectrum decomposition. Results are given in table 3. The comparison of calculated and experimental energy values has revealed that the wide strong resonances E_1 and E_3 are due to the transitions inside the octahedral sub-lattice, and the weak resonance of the opposite sign E_2 is associated with transition between tetrahedral and octahedral sub-lattices.

4. Conclusion

Monodispersed Fe_3S_4 spinel nanocrystals have been synthesized by the polyol mediated process, a modification of which enabled the synthesis of isostructural Fe_3O_4 nanocrystals of identical average size. We have performed a comparative experimental study of the Mössbauer spectra of the Fe_3S_4 and Fe_3O_4 nano-sized crystals and magneto-optical spectra of the transparent composite samples containing these nanocrystals as well as the theoretical study of the Fe_3S_4 electronic structure. The Fe_3O_4 Mössbauer spectrum demonstrates the Verwey transition, and the estimated value of the Verwey point, T_V, in this sample is 136 K. The shape of the Fe_3S_4 Mössbauer spectra and the hyperfine parameters indicate an absence of the Verwey transition at temperatures between 90 and 300 K. Analysis of the Mössbauer spectra allows showing the fast electron hopping between Fe^{2+} and Fe^{3+} ions in the B-sites and presenting the average iron valence to be near $Fe^{2.5+}$ for Fe_3S_4 at all temperatures between 90 and 300 K, but only at $T > T_V$ for Fe_3O_4. The magnetic circular dichroism (MCD) spectrum of Fe_3S_4 distinguishes drastically from that of Fe_3O_4. Most noticeable details in the Fe_3S_4 MCD spectrum are: (i) an absence of the negative peak observed in the MCD spectrum of Fe_3O_4, and (ii) the greater degree of the MCD signal increase in the vicinity of maximum at 2.0 eV comparing to that at 3.0 eV with the sample cooling. In order to extract meaningful information from the MCD data, we have carried out the MCD spectra decomposition to several Gauss-shaped components and identified the component energies with the transitions between the Fe_3S_4 energy states obtained from the *ab initio* band structure calculations.

Acknowledgments

We thank the National Science Council of Taiwan (NSC 100-2923-M-153-001-MY3 and NSC 102-2112-M-153-002-MY3) for financial support. Support by the Russian Foundation for Basic

Research (Grants #14-12-00848 and 14-02-0121) is acknowledged. This work was also supported by the Russian Federation President Grant NSh-2886.2014.2.

References

[1] Burda C, Chen X B, Narayanan R and El-Sayed M A 2005 *Chem. Rev.* **105** 1025
[2] Lu A-H, Salabas E L and Ferdi Schuth F S 2007 *Angew. Chem.* **46** 1222
[3] Hazra S and Ghosh N N 2014 *J. Nanosci. and Nanotechnol.* **14** 1983
[4] Baaziz W, Pichon B P, Fleutot S, Liu Y, Lefevre C, Greneche J M, Toumi M, Mhiri T and Begin-Colin S 2014 *J. Phys. Chem.* C **118** 3795
[5] Koralewski M, Kłos J W, Baranowski M, Mitróová Z, Kopčanský P, Melníková L, Okuda M and Schwarzacher W 2012 *Nanotechnology* **23** 355704
[6] Johnson C E, Costa L, Johnson J A, Brown D E, Somarajan S, He W and Dickerson J H 2014 *J. Phys. D: Appl. Phys.* **47** 075001
[7] He W, Osmulski M E, Lin J, Koktysh D S, McBride J R, Parke J-H and Dickerson J H 2012 *J. Mater. Chem.* **22** 16728
[8] He W, Somarajan S, Koktysh D S and Dickerson J H 2011 *Nanoscale* **3** 184
[9] Hasegawa Y, Kumagai M, Kawashima A, Nakanishi T, Fujita K, Tanaka K and Fushimi K 2012 *J. Phys. Chem.* C **116** 19590
[10] Skinner B J, Erd R C and Grimaldi F S 1964 *Am. Mineral* **49** 543
[11] Roberts A P, Chang L, Rowan C J, Horng C-S and Florindo F 2011 *Rev. Geophys.* **49** 46
[12] Fleet M E 1981 *Acta Crystallographica Section B-Struct. Sci.* **37** 917
[13] Chang L, Roberts A, Tang A Y, Rainford B D, Muxworthy A R and Chen Q J 2008 *Geophys. Res.* **113** B06104
[14] Aragón R 1992 *Phys. Rev.* B **46** 5328
[15] Uhl M and Siberchicot B 1995 *J. Phys.: Condens. Matter* **7** 4227
[16] Beal J H L, Prabakar S, Gaston N, Teh G B, Etchegoin P G, Williams G and Tilley R D 2011 *Chem. Mater.* **23** 2514
[17] Roldan A, Santos-Carballal D and de Leeuw N H J 2013 *Chem. Phys.* **138** 204712
[18] Lyubutin I S, Lin C R, Korzhetskiy Yu V, Dmitrieva T V and Chiang R K 2009 *J. Appl. Phys.* **106** 034311
[19] Lyubutin I S, Alkaev E A, Korzhetskiy Y V, Lin C R and Chiang R K 2009 *Hyperfine Interact.* **189** 21
[20] Lyubutin I S, Starchikov S S, Lin C-R, Lu S-Z, Shaikh M O, Funtov K O, Dmitrieva T V, Ovchinnikov S G, Edelman I S and Ivantsov R 2013 *J. Nanopart. Res.* **15** 1397
[21] Fontijn J W F, Van der Zaag P J, Devillers M A C, Brabers V A M and Metselaar R 1997 *Phys. Rev.* B **56** 5432
[22] Schlegel A, Alvarado S F and Wachter P 1979 *J. Phys. C: Solid State Phys.* **12** 1157
[23] Zhang X, Schoenes J and Wachter P 1981 *Solid State Commun.* **39** 189
[24] Antonov V N, Harmon B N, Antropov V P, Perlov A Y and Yaresko A N 2001 *Phys. Rev.* B **64** 134410
[25] Antonov V N, Bekenov L V and Yaresko A N 2011 *Adv. Condens. Matter Phys.* **2011** 298928
[26] Barnakov Y A, Scott B L, Golub V, Kelly L, Reddy V and Stokes K L 2004 *J. Phys. Chem. Solids* **65** 1005
[27] Smith D A, Barnakov Y A, Scott B L, White S A and Stokes K L 2005 *J. Appl. Phys.* **97** 504
[28] Neal J R, Behan A J, Mokhtari A, Ahmed M R, Blythe H J, Fox A M and Gehring G A 2007 *J. Magn. Magn. Mater.* **310** 246
[29] Gehring G A, Alshammari M S, Score D S, Neal J R, Mokhtari A and Fox A M 2012 *J. Magn. Magn. Mater.* **324** 3422
[30] Hoffmann V 1992 *Phys. Earth Planet. Inter.* **70** 288
[31] Scott G B, Lacklison D E, Ralph H I and Page J L 1975 *Phys. Rev.* B **12** 2562

[32] Lin C-R, Chiang R-K, Wang J-S and Sung T-W 2006 *J. Appl. Phys.* **99** 08N710
[33] Spender M R, Coey J M D and Morrish A H 1972 *Can. J. Phys.* **50** 2313
[34] Coey J M D, Spender M R and Morrish A H 1970 *Solid State Commun.* **8** 81605
[35] Zvezdin A K and Kotov V A 1997 *Modern Magnetooptics and Magnetooptical Materials* (Bristol and Philadelphia: IOP Publishing)
[36] deKronig R L J 1926 *Opt. Soc. Am.* **12** 547
[37] Kramers H A 1927 *Atti Cong. Intern. Fisica (Trans. of Volta Centenary Congress)* **2** 545
[38] Kresse G and Joubert D 1999 *Phys. Rev.* B **59** 1758
[39] Laasonen K A, Pasquarello R C, Lee C and Vanderbilt D 1993 *Phys. Rev.* B **47** 10142
[40] Perdew J P and Wang Y 1992 *Phys. Rev.* B **45** 13244
[41] Kresse G and Hafner J 1993 *Phys. Rev.* B **47** 558
[42] Kresse G and Furthmoller J 1996 *Phys. Rev.* B **54** 11169
[43] Vanderbilt D 1990 *Phys. Rev.* B **41** 7892
[44] Monkhorst H J and Pack J D 1976 *Phys. Rev.* B **13** 5188
[45] Devey A J, Grau-Crespo R and de Leeuw N H 2009 *Phys. Rev.* B **79** 195126
[46] Zhang B, de Wijs G A and de Groot R A 2012 *Phys. Rev.* B **86** 020406
[47] Anisimov V I, Aryaseriawan F and Lichtenstein A I 1997 *J. Phys.: Condens. Matter.* **9** 767